Potassium doping of single crystalline pentacene thin film

Fabio Bussolotti,* Satoshi Kera, and Nobuo Ueno†
Graduate School of Advanced Integration Science, Chiba University, Chiba 263-8522, Japan
(Received 9 August 2012; published 10 October 2012)

The impact of potassium (K) doping on the electronic structure of single crystalline pentacene (Pn) thin film grown on Cu(110) was investigated by high-sensitivity angle-resolved ultraviolet photoemission spectroscopy for K_xPn_1 ($0 \leqslant x \leqslant 1$). At room temperature (293 K), we observed that (i) Pn electronic states shift toward the high binding side with progressive growth of a gap state with the K-doping level, (ii) the highest-occupied molecular-orbital band dispersion of the pristine Pn SC multilayer survives perfectly even at the K-doping level of $x = 1$, and (iii) no dispersion occurs for the K-induced gap state. At 50 K, on the other hand, we found a small but clear dispersion (width ∼0.08 eV) of the K-induced gap state for the K_1Pn_1 SC multilayer, which is in good agreement with theoretical prediction on the band structure of K_1Pn_1 Mott-Hubbard insulator crystal. This finding demonstrates that the K-induced gap state originates from the Mott-Hubbard insulator formed by electron transfer from the K atom to Pn lowest-unoccupied molecular orbital. The Hubbard energy U was estimated to be ∼2 eV at 293 and 50 K, which is also in fairly good agreement with the theoretical value of 1.5 eV. Moreover, significant density of states at the Fermi level, which is related to a metallic phase for the metal-insulator transition, could not be detected for the doping level of $0 \leqslant x \leqslant 1$. This indicates that the Mott-Hubbard insulator ground state is stable for $0 \leqslant x \leqslant 1$ and does not show x-dependent metal-insulator transition at least near the surface region. The impact of K doping on the energy-level alignment was discussed in terms of coexistence of K_1Pn_1 Mott-Hubbard insulator and Pn SC film.

DOI: 10.1103/PhysRevB.86.155120 PACS number(s): 79.60.Fr, 68.55.Ln, 71.30.+h, 81.05.Fb

I. INTRODUCTION

Organic semiconductors have attracted considerable interest as promising base materials for optoelectronic devices.[1–3] For any applicative purpose, a complete control on the charge transport properties of organic films is a mandatory step. In this context, $n(p)$-type doping via intercalation of alkali metal atoms represents an efficient strategy for enhancing the electrical conductivity of organic materials,[4–7] Many theoretical and experimental investigations were, therefore, focused on the electronic properties of alkali-doped organic systems.[8–14] Among organic systems, alkali-doped conjugated polymer and fullerene films have been extensively studied for many years.[15–21] In contrast, the nature of the alkali doping into smaller π-conjugated molecular systems with weak intermolecular interaction remained relatively unclear and less explored, although a possibility of strong electronic correlation effects,[22] for example, the effects of large onsite Coulomb repulsive energy, may also be expected in these molecular systems, due to wave-function localization at each molecular site.

An insulator-metal-insulator transition as a function of doping was recently observed in transport studies on alkali n-doped phtalocyanine and pentacene thin films.[6,7] The initial increase of electrical conductivity was attributed to the filling of the lowest-unoccupied molecular orbital (LUMO) by electrons from alkaline atoms. At higher doping levels, the organic films become insulators due to electron-phonon coupling or electronic correlation effects.[6,7,13] These results are in contrast with ultraviolet photoelectron spectroscopy (UPS) studies on nominally equivalent alkali-doped films.[10,11,14] In particular, no detectable density of states (DOS) was observed at the Fermi level, indicating that the organic films were in a stable insulating state.[10,11,14] Such an inconsistency was tentatively attributed to structural differences among doped organic films.[23] The electronic properties of organic semiconductors, in fact, strongly depend on the intermolecular packing due to the planar molecular structure.[24] Moreover, UPS investigations were mainly conducted on polycrystalline or amorphous alkali-doped organic thin films.[5,9–11,14] A large concentration of structural defects (i.e., grain boundaries, molecular vacancies) limits the diffusion of dopants within the organic layer[25] and leads to an inhomogeneous distribution of dopants in the organic films. An imperfect molecular packing structure mediated by inhomogeneity of the alkali atom distribution may cause, in principle, site dependence of the intermolecular electronic coupling and the relaxation/polarization energy, which leads to broadening of UPS bandwidth[26,27] and electronic states in the band gap that affects the energy-level alignment (ELA) at organic/metal interfaces.[28–30] Despite the importance of minimizing structural imperfections to reach the nature of K-induced electronic properties, UPS studies on doped single crystalline (SC) multilayers of small π-conjugated molecules remained mainly marginal.[31]

In this paper we report on the electronic properties of potassium- (K-) doped SC thin film of pentacene (Pn) prepared on Cu(110) studied by angle-integrated and resolved UPS techniques. The impact of K doping on the electronic band structure of Pn SC thin film was carefully evaluated. We found that the band dispersion of the highest-occupied-molecular-orbital (HOMO) states of the pristine Pn SC thin film stayed unchanged in the K_1Pn_1 SC thin film at room temperature (293 K), while the K-doping-induced gap state appeared. At 50 K, a band dispersion (∼0.08 eV) of the gap state was clearly observed for the K_1Pn_1, which is in fairly good agreement with the theoretical prediction for K_1Pn_1 Mott-Hubbard insulator single crystal. The K-induced gap state was finally identified as the occupied Mott-Hubbard band of the K_1Pn_1 Mott-Hubbard insulator. The role of the Mott-Hubbard insulator is discussed in relation to the ELA.

II. EXPERIMENTAL

High-purity (99.999%) Cu(110) single crystal was repeatedly cleaned by a series of sputtering-annealing cycles. The quality of the surface was checked by preliminary angle-resolved UPS (ARUPS) investigations. Pn molecules ($C_{22}H_{14}$; Sigma Aldrich), purified by three cycles of vacuum sublimation, were vacuum deposited onto the Cu(110) clean substrate according to the two-step procedure described in Ref. 32: at the first step, a saturated flat-lying Pn monolayer was grown at a substrate temperature of 450 K; in the second step, the Pn monolayer was used as a template to grow an upright-standing SC Pn multilayer at 320 K [Fig. 1(a)]. According to Lukas *et al.*,[32] the SC structure of the Pn film is characterized by a surface rectangular unit cell of 5.8 and 7.4 Å along the [1-10] and [001] substrate directions, respectively. These lattice values were confirmed by the present Pn films by the ARUPS data reported in the present work. A schematic representation of the surface Brillouin zone (SBZ) of the Pn SC multilayer is shown in Fig. 1(b). Film thickness and deposition rate (0.1 nm/min) were monitored by using a quartz microbalance. During the deposition, the pressure was stably lower than 4×10^{-8} Pa.

After the growth of the Pn multilayer, potassium (K) metal atoms were deposited at 293 K from carefully outgassed dispensers (SAES Getters S.p.A.). During K deposition, the pressure in the preparation chamber remained below 5×10^{-8} Pa. The total number of K atoms per Pn molecule (referred as doping level x) was evaluated from the K2p and C1s core level intensity ratio measured by x-ray photoemission spectroscopy (XPS) with Al K_α ($h\nu = 1486.6$ eV), where the ratio was calibrated with respect to (i) the number of C atoms per Pn molecule and (ii) C1s and K2p photoionization cross sections at a photon energy of 1486.6 eV ($\sigma_{C1s}/\sigma_{K2p} \sim 0.25$).[33]

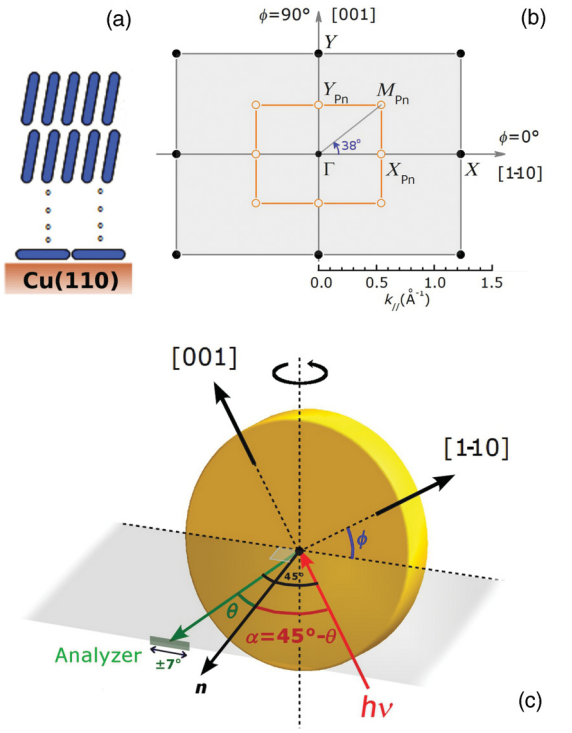

FIG. 1. (Color online) (a) Schematic representation of the upright-standing Pn multilayer film structure. (b) Sketch of the SBZ of upright-standing Pn multilayer film on Cu(110). (c) Experimental parameters of photoelectron experiment: the photon incidence angle α, electron takeoff angle θ, and sample azimuthal angle ϕ.

UPS experiments were performed by using high-sensitivity, ultralow background apparatus with a hemispherical electron energy analyzer (MBS A-1) and a monochromatic He I_α ($h\nu = 21.218$ eV) radiation source. Further details on the experimental apparatus may be found in Ref. 30. A complete definition of the UPS experimental geometry, including photon incidence angle (α), photoelectron emission angle (θ), and the sample azimuthal angle (ϕ) is shown in Fig. 1(c). The binding energy scale was measured with respect to the Fermi level of the substrate. For both angle-integrated and resolved UPS, the total energy resolution was set to 30 meV. Angle-integrated spectra were acquired at normal emission ($\theta = 0°$) with an integration angle of $\pm 7°$, where a bias of -5 V was applied to the sample to measure the vacuum level (VL). In the ARUPS the angle-resolving range spanned $\pm 7°$ with respect to the lens axis, and angular resolution was set to 1°. Wider angular dependence was accessed by rotating the sample with respect to the lens axis. No bias was applied to the sample during ARUPS measurements.

K was deposited until the saturation of the VL shift, where the doping level corresponded to $x = 1$. K deposition was then stopped in order to safely avoid the formation of K metallic clusters. Spectral broadening due to charging effects of the films were not observed during the UPS measurements for both the pristine and K-doped Pn films, as judged from observation of a very sharp cutoff of the secondary electrons as well as small band dispersions.

III. RESULTS AND DISCUSSION

A. Impact of K doping on the film structure and energy levels

Figure 2 shows the 293 K-He I_α UPS (angle-integrated) spectra of the Pn/Cu(110) multilayer (8 nm) as a function

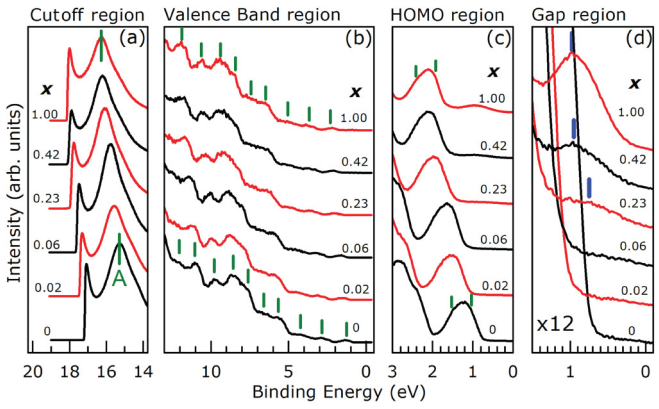

FIG. 2. (Color online) He I_α UPS spectra (angle integrated) of Pn/Cu(110) multilayer (8 nm) as a function of K-doping level (x) in the secondary electron cutoff (a), valence band (b), HOMO (c), and band-gap (d) regions. All of the spectra were measured at 293 K. The binding energy scale refers to the Fermi level of the substrate. Pn-related features are indicated by vertical bars.

of x. All Pn-related UPS features are indicated by vertical bars. For the pristine Pn film, an intense peak (A) was observed in the secondary electron region [Fig. 2(a)].[34] Such features in photoemission spectra are generally related to electronic states above the VL.[26] For pentacene, feature A is associated to a high DOS in the conduction band of ordered films with an upright-standing molecular orientation.[26] The upright-standing configuration is generally accompanied by a herringbone-type arrangement within the layers parallel to the substrate surface.[35,36] The same intermolecular packing geometry was observed for the (001) plane of Pn single crystals.[37]

A clear energy splitting of the HOMO level was observed [Fig. 2(c)]. The two HOMO features originate from the DOS structure due the intermolecular HOMO band dispersions with the presence of two nonequivalent molecules in the unit cell.[26,35,36,38–40]

As K atoms were deposited onto the Pn SC film at 293 K, the VL and Pn-related UPS features progressively shifted toward the higher binding energy side [Figs. 2(a)–2(c)]. At the same time, a new spectral feature appeared in the gap region [Fig. 2(d)]. For both the HOMO and the gap state, we found that full width at half maximum (FWHM) was (0.60 ± 0.05) eV. Moreover, we did not observe any steplike feature and/or tailing for the secondary electron cutoff but a very sharp cutoff that reaches the baseline directly for the K-doping level of $0 \leqslant x \leqslant 1$, suggesting that the film is uniform even after K doping [Fig. 2(a)].

The K doping did not introduce any significant broadening of the spectral features. This is not generally observed in UPS investigation on alkali doping of polycrystalline and amorphous organic thin film.[10,11,14,31] Structural defects in the films limit uniform dopant diffusion, and thereby imperfect film structures are induced more to result in serious broadening of UPS features. Note that no such changes were detected for the HOMO conduction band, feature A and the secondary electron cutoff [Figs. 2(a) and 2(c)], all of which are sensitive to the film structure.[26,40] It is, therefore, concluded that the K doping did not significantly affect the molecular orientation, and the intermolecular packing geometry, i.e., the present Pn multilayer kept the SC structure upon K doping. This result suggests that K atoms are intercalated *between* the Pn-stacking layers, which is in agreement with theoretical studies on K_1Pn_1 SC structure.[7]

Polaron formation due to electron transfer from alkaline atoms to molecules is commonly invoked to explain the gap states in alkali doped organic films.[15,41,42] In the present K-doped Pn SC multilayer, the gap-state formation must be interpreted differently. In alkali-doped organic systems, in fact, polaron formation leads to a significant change in the binding energy of the frontier orbitals, where an increase (∼0.2–0.3 eV) in the HOMO binding energy was observed.[15,41,42] If this is also the case for the present K-doped Pn SC multilayer, the presence of the Pn molecule in a different charging state (i.e., with different HOMO binding energy) should result in a broadening of the HOMO line shape at low- and intermediate-doping levels ($0 < x < 1$). The stability of the HOMO line shape of the Pn SC multilayer upon K doping clearly indicates the absence of polaron formation due to electron transfer from K atoms to Pn molecules. As shown in Fig. 3, the K-induced binding energy shift is the same for the HOMO and the VL (Fig. 3). Such a "rigid" energy shift also indicates the absence of polaron formation.[43]

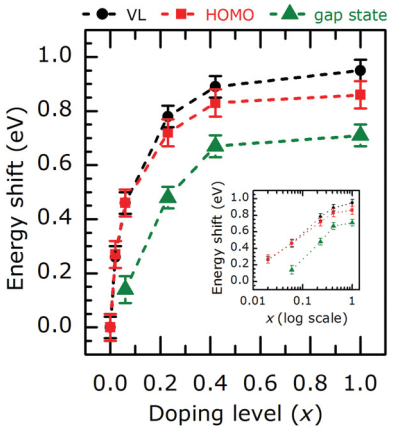

FIG. 3. (Color online) Summary of the doping-induced binding energy shift of VL (black circle), HOMO peak position (red square), and gap state peak position (green triangle). For the gap state, the energy shift was evaluated with respect to the position at $x = 0.02$. The VL and HOMO energy shifts are coincident within experimental error. The inset displays a semilogarithmic plot in order to show the linear dependence of the energy shift on $\ln(x)$ (see text for discussion).

For K_1Pn_1 SC, the Mott-Hubbard metal-insulator transition was theoretically predicted by Craciun *et al.*[7] In K_1Pn_1 SC, Pn LUMO band is half filled, which corresponds, in principle, to a metallic phase. However, the strong electron-electron correlations determine the splitting of the half-filled LUMO band into unoccupied (above the Fermi level) and occupied (below the Fermi level) bands. K_1Pn_1 is, therefore, driven into an insulating state to become a Mott-Hubbard insulator.[7] The electronic correlation effects are enhanced by the low value of the LUMO bandwidth (W) with respect to the onsite Coulomb repulsion energy U ($U/W \sim 2.1$[7]). For the present K-doped Pn SC multilayer, the Mott-Hubbard transition can explain the origin of the gap state, which can be identified as the occupied Mott-Hubbard band as discussed in the next section. It is also worth to note here that (i) according to theoretical study of the K_1Pn_1 Mott-Hubbard insulator, K-derived states present only at much higher energy above the Fermi level, suggesting that the role of the potassium atoms is limited to transferring their electrons to the pentacene molecules[7] and (ii) the stability of binding energy of valence band states upon the Mott-Hubbard transition is commonly observed for inorganic compounds.[44,45]

B. Band dispersion and formation of Mott-Hubbard insulator

In order to evaluate the impact of the K doping on the intermolecular interaction, the degree of charge delocalization, and electronic correlation, the band structure of pristine Pn and K_1Pn_1 SC films were measured by ARUPS. The results at 293 K are summarized in Figs. 4 and 5.

Figure 4(a) shows the θ dependence of ARUPS in the HOMO region of the pristine Pn and K_1Pn_1 films along $\Gamma-X_{Pn}$, $\Gamma-Y_{Pn}$, and $\Gamma-M_{Pn}$ directions of the Pn SBZ [see Fig. 1(b)]. As seen in the figure, ARUPS spectra are

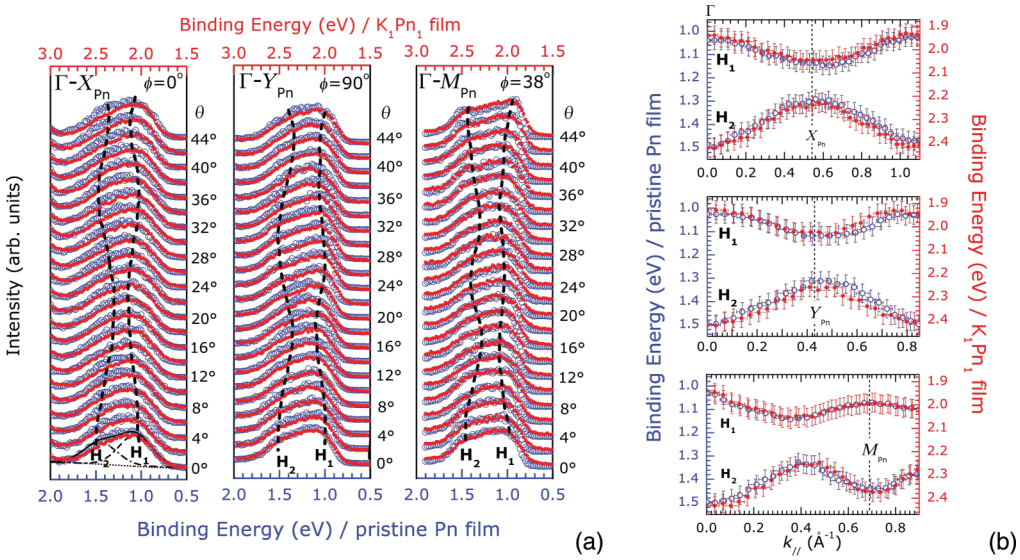

FIG. 4. (Color online) (a) θ dependence of ARUPS spectra for pristine Pn [open (blue/medium gray) circles] and K_1Pn_1 [closed (red/dark gray) circles] SC films, as acquired at $\phi = 0^\circ$ ($\Gamma-X_{Pn}$ direction), $\phi = 90^o$ ($\Gamma-Y_{Pn}$ direction), and $\phi = 38^o$ ($\Gamma-M_{Pn}$ direction). All data were acquired at 293 K. The binding energy positions of the HOMO-derived states (H_1 and H_2) are indicated by dashed lines. H_1 and H_2 positions were determined by the least-square fitting of the ARUPS data by using Gaussian functions on a linear background. An example of ARUPS data fitting is shown for pristine Pn film at $\theta = 0^\circ$ and $\phi = 0^\circ$ (dash-dotted lines = Gaussian components, dotted line = linear background, continuous line = cumulative fitting curve). Lower (blue/medium gray) and upper (red/dark gray) binding energy scale are for pristine Pn and K_1Pn film, respectively. (b) HOMO-band dispersion, $E_B(k_\parallel)$, for pristine Pn [open (blue/medium gray) circles] and K_1Pn [closed (red/dark gray) circles] along the $\Gamma-X_{Pn}$ direction (upper panel), $\Gamma-Y_{Pn}$ direction (middle panel), and $\Gamma-M_{Pn}$ direction (lower panel). Left (blue/medium gray) and right (red/dark gray) binding energy scales are for pristine Pn and K_1Pn_1 multilayer, respectively.

independent of the K doping. In particular, for both films, the H_1 and H_2 features are clearly visible at $\theta = 0^\circ$. These peaks gradually disperse with θ, as highlighted by dashed curves superimposed to the ARUPS data. Peak positions were determined by the least-square fitting of the ARUPS data by using Gaussian functions on a linear background. Along the $\Gamma-X_{Pn}$ ($\Gamma-Y_{Pn}$), the energy separation is progressively reduced to reach minimum value at $\theta = 16^\circ$ ($\theta = 14^\circ$). At higher θ, the splitting increases again until $\theta = 32^\circ$ ($\Gamma-X_{Pn}$) and $\theta = 28^\circ$ ($\Gamma-Y_{Pn}$), where the normal emission HOMO line shape is basically recovered. Along the $\Gamma-M_{Pn}$, similar behavior was observed with the dispersion turning points located at around $\theta \sim 22^\circ$ and $\theta \sim 44^\circ$. The band dispersions, $E_B(k_\parallel)$ of H_1 and H_2 peaks for pristine and doped films are plotted in Fig. 4(b), where $k_\parallel$ represents the component of the photoelectron wave vector parallel to the surface. The observed H_1 and H_2 band dispersions of the undoped Pn are in good agreement with previous experimental results[38] and *ab initio* calculations for the Pn bulk phase.[24] Note that for both films and along all symmetry directions, H_1 and H_2 states disperse similarly. The ARUPS band dispersions of the pristine and K-doped films coincided in terms of the bandwidth and dispersion phase [Fig. 4(b)]. The turning points of $E_B(k_\parallel)$ curves exist at $k_\parallel = (0.54 \pm 0.02)$ Å^{-1}, $k_\parallel = (0.42 \pm 0.02)$ Å^{-1}, and $k_\parallel = (0.69 \pm 0.02)$ Å^{-1} along the $\Gamma-X_{Pn}$, $\Gamma-Y_{Pn}$, and $\Gamma-M_{Pn}$ directions, respectively. These values are in excellent agreement with those evaluated from the Pn unit cell lattice parameters,[32] i.e., $kth_\parallel = 0.542$ Å^{-1} (along $\Gamma-X_{Pn}$), $kth_\parallel = 0.425$ Å^{-1} (along $\Gamma-Y_{Pn}$), and $kth_\parallel = 0.688$ Å^{-1} (along $\Gamma-M_{Pn}$). Such agreement confirms that the pristine and K-doped Pn multilayers have SC structure. The stability of the band dispersion upon K doping further demonstrates that K atoms are not intercalated among the standing Pn molecules within each stacking layer but between the Pn-stacking planes. This conclusion is reasonable, since it is expected that the theoretically predicted increase of the plane separation (~8%) upon K doping[7] does not significantly affect the film electronic structure due to much weaker intermolecular interaction between adjacent Pn layers than within each Pn layer.

Figure 5 shows the ARUPS results for the gap state in the K_1Pn_1 multilayer. No clear band dispersion was detected along the main symmetry directions of the surface unit cell, i.e., the gap state is well localized at 293 K. The differences between the dispersion widths of the gap state and the HOMO can be due to different spatial distribution of wave functions of these states. For Pn SC film intercalated with Rubidium (Rb) layers (Rb_1Pn_1), the wave function of the gap state was predicted to be localized at the edges of Pn molecules and near to the alkaline atom plane,[46] limiting intermolecular $\pi-\pi$ interaction.

ARUPS investigation was also conducted on the K_1Pn_1 film at 50 K. Figure 6(a) shows the ARUPS results for the HOMO region, as acquired along the $\Gamma-M_{Pn}$ direction. In contrast to the 293-K results, clear HOMO band splitting as well as dispersion was not observed at 50 K although θ-dependent band shape was found. The temperature-dependent change in the spectral shape of the HOMO band can be ascribed to a temperature-induced change in intermolecular packing structure. It was pointed out theoretically[24] and experimentally[40] that a slight change in the film structure, in fact, seriously affects the electronic band structure. For the gap state, on the other hand, a small but clear band dispersion (~0.08 eV) was observed along the $\Gamma-M_{Pn}$ direction as shown in Fig. 6(b).

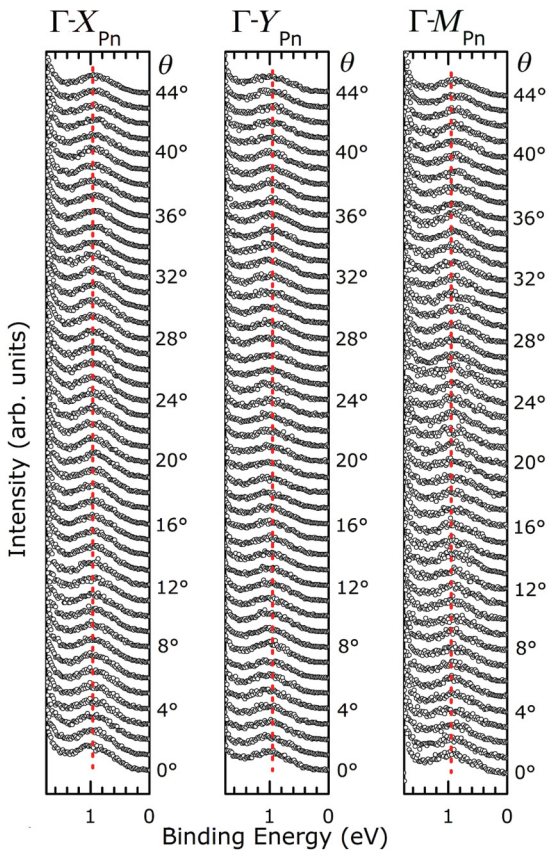

FIG. 5. (Color online) θ dependence of ARUPS spectra for the gap state in K_1Pn_1 SC film at 293 K, as acquired along $\Gamma-X_{Pn}$, $\Gamma-Y_{Pn}$, and $\Gamma-M_{Pn}$ directions. Dashed (red) lines indicate the gap-state peak position. No energy dispersion was detected.

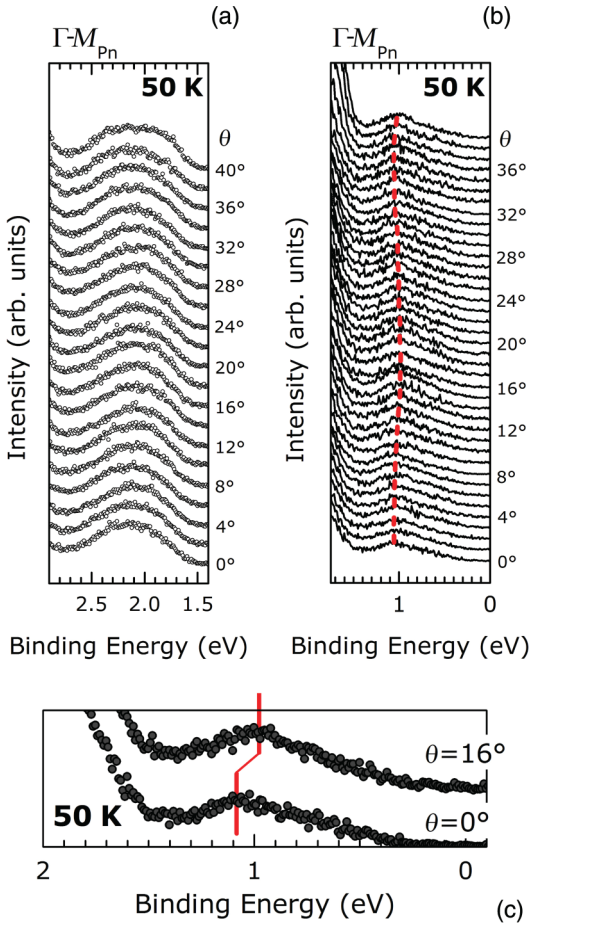

FIG. 6. (Color online) θ dependence of ARUPS spectra for HOMO (a) and gap state (b) in K_1Pn_1 SC film at 50 K, as acquired along the $\Gamma-M_{Pn}$ direction. (c) Comparison between the spectra at $\theta = 0^\circ$ and $\theta = 16^\circ$ to clearly show the binding energy change due to the dispersion.

The existence of such a dispersive behavior was confirmed, as shown in Fig. 6(c), where the energy difference of the gap-state positions at $\theta = 0^\circ$ and $\theta = 16^\circ$ (i.e., dispersion turning points) is highlighted. The band dispersion of the gap state also demonstrates that the K_1Pn_1 film keeps the SC structure. Figure 7(a) displays the experimental band dispersion of the K_1Pn_1 film along $\Gamma-M_{Pn}$. The dispersion can be quantitatively discussed within the framework of a simple one-dimensional tight-binding model: $E_B(k_\parallel) = E_c - 2t\cos(\pi k_\parallel/G)$[40] where E_c is the energy of the band center, t is the transfer integral, and G is the size of the SBZ. The best fit of the experimental data with a cosine curve is shown in Fig. 7(c) and gives $E_c = (1.021 \pm 0.003)$ eV, $t = (0.020 \pm 0.003)$ eV, and $G = (0.62 \pm 0.01)$ Å^{-1}. In particular, at 50 K, the symmetry turning point of the gap-state band (M_{Pn}^{50K},) was experimentally found at 0.62 Å^{-1} [Fig. 7(a)], which is located closer to the Γ point than that observed at 293 K ($\Gamma-M_{Pn} = 0.69$ Å^{-1}, as evaluated from the HOMO band dispersion at 293 K). The observed contraction of the SBZ at 50 K [see inset in Fig. 7(a)] corresponds, in real space, to an increase of ~10 and ~12% in the size of the unit cell along the [1–10] and [001] directions, respectively. This result supports the occurrence of temperature-induced change in the intermolecular Pn-packing structure. Interestingly, similar lattice expansion after alkaline doping was recently reported for cesium- (Cs-) doped Pn thin film by Annese *et al.*[31] (see end of the Sec. B). In order to determine the lattice parameters of K_1Pn_1 SC unit cell at 50 K more precisely, accurate structural investigations are required.

Figure 7(b) shows the theoretical band dispersion for the low Mott-Hubbard band of K_1Pn_1 Mott-Hubbard insulator crystal, as evaluated along the $\Gamma-M_1$ and $\Gamma-M_2$ directions (adapted from Ref. 7). The two directions, $\Gamma-M_1$ and $\Gamma-M_2$, are defined for the SBZ of the K_1Pn_1 crystal used in calculations[7] [see inset in Fig. 7(b)]. M_1 and M_2 come from slightly different crystal structure used in the calculation and $M_1 = M_2$ in the present crystal structure [rectangular SBZ, see Fig. 1(b)]. Interestingly, at 50 K, the experimental band dispersion [Fig. 7(a)] along the $\Gamma-M_{Pn}$ direction agrees well with the theoretical prediction [Fig. 7(b)] if we consider $M_1 = M_2$, both in term of bandwidths and dispersion phase. This agreement further indicates that the Mott-Hubbard insulator can be the origin of the gap state in the K-doped Pn SC thin film.

Here we compare the present results with those reported recently for Cs-doped flat-lying Pn SC film on Cu(119) by Annese *et al.*[31] They found that the Cs deposition on the flat-lying Pn film determined variation of the overall UPS spectral line shape. At room temperature, ARUPS revealed the formation of a new LUMO-derived state at ~0.6–0.7 eV

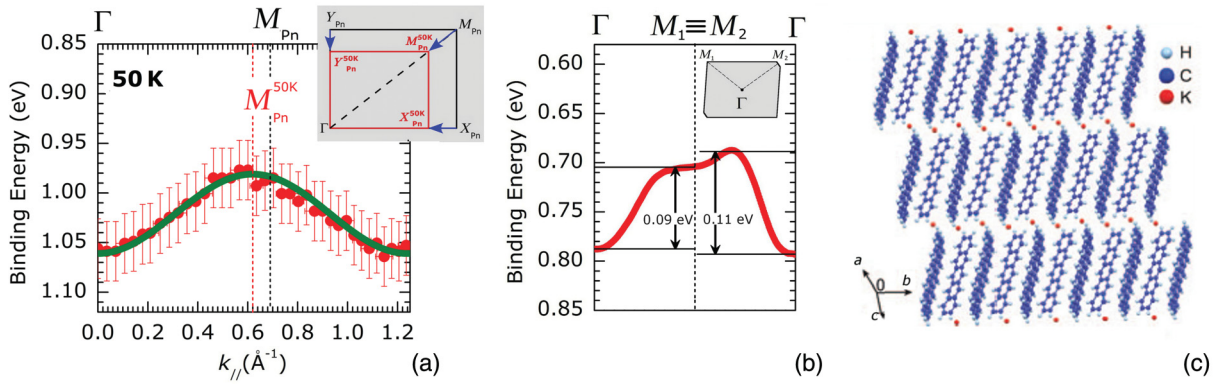

FIG. 7. (Color online) (a) Band dispersion, $E_B(k_\parallel)$, of the gap state along the $\Gamma-M_{Pn}$ direction at 50 K. Solid (green) line represents tight-binding fit of the experimental data [filled (red) circles]. The SBZ edges at 50 K (M^{50K}_{Pn}) and at 293 K (M_{Pn}) are indicated by dotted lines. The rectangular SBZ at RT and its shrinkage at 50 K are schematically illustrated in the inset (see text for detailed discussion). (b) Theoretical band dispersion of lower Mott-Hubbard band along $\Gamma-M_1$ and $\Gamma-M_2$ directions of the SBZ of K_1Pn_1 Mott-Hubbard insulator crystal (data adapted from Ref. 7). Sketch of SBZ of the K_1Pn_1 Mott-Hubbard insulator crystal used in calculations in Ref. 7 is shown in the inset of panel (b). M_1 and M_2 come from slightly different crystal structure used in the calculation and $M_1 = M_2$ in the present crystal structure [rectangular SBZ, see Fig. 1(b)]. Experimental dispersion of the gap state [panel (a)] agrees well with the theoretical result (after averaging the curves along $\Gamma-M_1$ and $\Gamma-M_2$ directions) [panel (b)]. (c) Side view of the stacked layers of Pn and K in K_1Pn_1 SC film, illustrating the potassium intercalation in between the molecular planes (figure adapted from Ref. 7). Note that panel (c) represents the structure in the bulk of K_1Pn_1 SC film. In the present case of K_1Pn_1 multilayer, no K atoms are present on top of the surface Pn layer.

below the Fermi level. For their Cs_2Pn_1 film, a band dispersion (0.13 eV) of the gap state was observed at room temperature, while no dispersion was detected for the HOMO, along the direction perpendicular to the substrate surface. They also found that the periodicity of the gap state dispersion was related to an expansion of the lattice constant of 0.6 Å (i.e., ∼20%) along the molecular stacking direction (normal to the surface). The present results for K_1Pn_1/Cu(110) film agrees *qualitatively* with those of Cs_2Pn_1/Cu(119) film.[31] In particular, a large lattice expansion was observed after alkaline doping for both Pn/Cu(110) and Pn/Cu(119) SC thin film. The difference between Cs_2Pn_1 and the present K_1Pn_1 may originate from the different nature of the dopant species and structure of the pristine Pn film (flat lying vs upright standing).

C. Intensity of the gap state and its impact on ELA

In order to discuss the origin of the gap state in more detail and its impact on the ELA, angle-integrated UPS spectra around the gap state are shown on a log scale in Fig. 8 as a function of the K-doping level. The background contribution was removed, and the intensity was normalized as described in Ref. 30. In the pristine Pn SC film, a very tiny exponential tail (linear on the log scale of Fig. 8) is visible between the HOMO edge (∼0.7 eV) and the Fermi level (see shaded gray area in Fig. 8). Such a density of gap states was observed by Sueyoshi *et al.*[30] for Pn of Pn(standing orientation)-monolayer/ClAl-phthalocyanine/graphite, which originates from structural imperfections in the intermolecular packing that may be mediated by hole injection from the substrate into the Pn layer (positively charged polaron).[30]

Even for the $K_{0.02}Pn_1$ film, the K-induced gap states were clearly detected in the gap region (indicated by triangle marker in Fig. 8). The intensity of the gap states increases with K doping, and the peak position progressively shifts toward the higher binding energy side [see Figs. 2(d), 3, and 8]. No significant photoemission signal was detected at the Fermi level even for $x = 1$, indicating the stable insulating nature of the K-doped Pn film. In contrast, transport measurements on highly ordered K_xPn_1 film by Craciun *et al.*[7] suggested that an insulator-metal-insulator transition appeared depending on x. At the low- and intermediate-doping levels ($0 < x < 1$), they observed a sharp increase in the Pn film conductivity, resulting in a metallic behavior.[7] The metallic behavior was ascribed to the progressive filling of the LUMO with electrons donated from K atoms.[7] At $x = 1$, electron-electron interactions cause the splitting of the half-filled LUMO band and the opening of a Mott-Hubbard gap. The gap opening explained the observed reentrance of K_1Pn_1 film into an insulating state.[7] The evolution of UPS spectra for the present Pn/Cu(110) SC multilayer upon K doping can be rationalized in terms of coexistence of pristine Pn SC and K_1Pn_1 Mott insulator at any level of K doping. Similar phase separation phenomena were observed in K-doped fullerene films and attributed to the limited solubility of K atoms within the organic matrix host.[18]

For a brief summary of energy levels observed by the present experiment, impact of the phase coexistence on the ELA is illustrated in Fig. 9. For low- and intermediate-doping levels ($0 < x < 1$), the LUMO band is progressively filled with x and Mott-Hubbard transition occurs to form a small K_1Pn_1 Mott-Hubbard insulator, which yields a gap state below the Fermi level (middle panel in Fig. 9). The Mott-Hubbard-derived gap states act as electron "donor" levels, which can populate, via thermal excitation, the empty Pn LUMOs above the Fermi level. As K-doping level increases, a larger number of donor gap states become available thus leading to the gradual upward shift of the Fermi level (middle panel in Fig. 9). Finally, the x-dependent shift of Pn energy levels saturates when a continuous film of K_1Pn_1 is formed ($x = 1$) and the Fermi level is located at the middle of the Mott-Hubbard gap (right panel in Fig. 9).

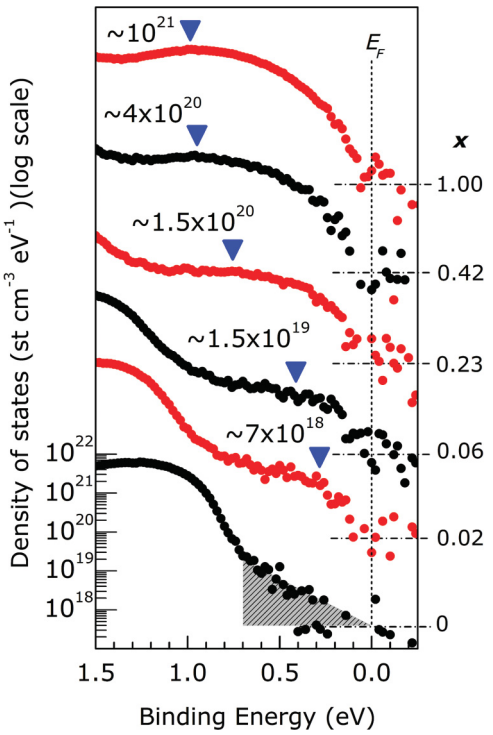

FIG. 8. (Color online) (a) The DOS deduced from He I_α UPS spectra (angle integrated) of Pn/Cu(110) multilayer as a function of K-doping level (x) in the HOMO-LUMO gap region. The spectra were acquired at 293 K. Background contribution was subtracted according to same procedure described in Ref. 30. The DOS is plotted on a log scale to show tiny K-induced DOS. The molecular packing density of the bulk phase of Pn (2.9×10^{21} cm^{-3}) was used to obtain DOS (states per cubic centimeter per electron volt), according to the same procedure described in Ref. 28 and 30. The molecular packing density was obtained from the lattice parameters reported in Ref. 24 for the Pn bulk phase. Peak position of the gap state is indicated by blue triangular markers [see also Fig. 2(d)]. Note that a clear increase in the DOS of gap states was observed even at the very beginning of the K-doping process ($x = 0.02$). DOS values at peak positions of gap states are shown in the figure. As the DOS values involve photoelectron attenuation effect, values 10 times larger must be considered for actual DOS (see discussion in the last part of the Sec. C).

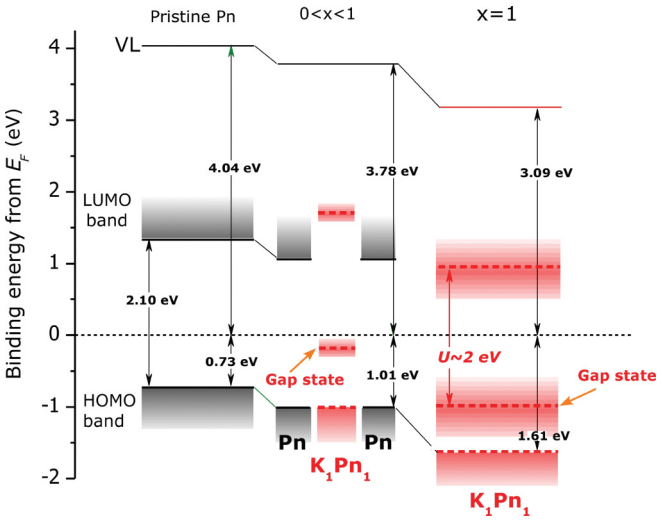

FIG. 9. (Color online) Summary of ELA in thin films with Pn and K_1Pn_1 phases at 293 K. Pn (K_1Pn_1) energy level and bandwidth are indicated by black (red/dark gray) line and by black (red/dark gray) shadow, respectively. The LUMO position for Pn SC film was taken from Ref. 29. At low- and intermediate-doping levels ($0 < x < 1$), Pn LUMO starts filling to give localized gap state below the Fermi level, which originates from the K_1Pn_1 Mott-Hubbard insulator. Note that the HOMO binding energies of pristine Pn and K_1Pn_1 crystals are the same for $0 < x < 1$ according to the UPS results (see text). The energies in the middle panel are shown for $x = 0.02$. At $x = 1$, a SC K_1Pn_1 Mott insulator is formed and the Fermi level (E_F) lies in the middle of the Hubbard energy gap U.

As shown in the inset of Fig. 3, energy level shifts depend linearly on the logarithm of doping level i.e., $\Delta E \propto \alpha k_B T \ln(x)$ for $x < 1$, where ΔE is the energy level shift, $k_B T$ is the thermal energy (~25 meV at 293 K), and α is a proportional coefficient. This is in agreement with the prediction of the classical theory of doping in a semiconductor.[10,47,48] In particular a value of $\alpha \sim 7$, $\alpha \sim 6$, and $\alpha \sim 8$ was determined for the VL shift, HOMO level shift, and gap-state energy shift, respectively. The α values of the VL and HOMO shifts are nearly the same, indicating that the energy shifts are mainly related to the Fermi level shift in the energy gap, while a larger α of the gap state may involve also size dependence of the K_1Pn_1 binding energy. Values of $\alpha > 1$ were similarly reported by Ding *et al.*[10,47] for Cs-*n*-doped phtalocyanine thin film. They suggested that the large value of α originates in the population of the LUMO tailing with electrons from the ionized donor atoms. The LUMO tailing in organic semiconductors can be related to the gap-state distribution sensitively originating from structural imperfection.[30]

According to the binding energy of the gap-state peak in the K_1Pn_1 SC film (0.98 eV at 293 K and 1.02 eV at 50 K), Hubbard energy U can be estimated to be ~2.0 eV at 293 and 50 K, which is in fairly good agreement with the theoretical value of $U = 1.5$ eV.[7] Within the framework of the ELA model in Fig. 9, the intensity of the gap state in UPS is expected to increase with K_1Pn_1 crystals size, as observed in Figs. 2(d) and 8. As already discussed in Sec. A, the opening of the Mott-Hubbard gap does not affect the binding energy position of the K_1Pn_1 HOMO level with respect to that of pristine Pn. This is illustrated in the middle panel of Fig. 9. At low- and intermediate-doping levels ($0 < x < 1$), a large difference between the HOMO positions of pristine Pn SC film and K_1Pn_1 should result in HOMO line-shape broadening, which was not observed in the photoelectron spectroscopy data [Figs. 2(c) and 4(a)].

Finally, we comment on much lower UPS intensity of the gap state than that of the HOMO for the K_1Pn_1 SC film. If we assume that (i) the wave function of the occupied Mott-Hubbard insulator state is localized near the interlayer boundary as predicted by theory[7,46] [see also Fig. 7(c)], i.e., near the bottom edges of upright-standing Pn molecules in the surface layer and (ii) K atoms do not exist at the surface, photoelectrons from the gap state are attenuated more than those from the HOMO distributed over each Pn molecule before escape to vacuum. The UPS intensity ratio between the HOMO (distributed over Pn molecule) and gap state (localized near the bottom edge of the first layer Pn), $I_{\text{gap state}}/I_{\text{HOMO}}$,

was estimated to be ∼0.1 for the K_1Pn_1 SC film by using the electron attenuation length (∼1 nm), the length of Pn molecule (∼1.5 nm), substantial wave-function spread of the Mott-Hubbard state (∼0.5 nm; localized on two aromatic rings near the bottom edge of Pn), and the number of electrons in the HOMO (two electrons) and the Mott-Hubbard insulator state (one electron). This ratio agrees well with the experimental ratio [∼0.12, see Fig. 2(d)].

IV. CONCLUSIONS

The electronic properties of K-doped SC Pn thin film were investigated by UPS. The impact of K doping on (i) the electronic band structure of the Pn thin film and (ii) ELA at the organic/substrate interface were carefully evaluated. At 293 K, a progressive shift of the Pn molecular states toward the high binding energy side was observed with increase in the K-doping level. At the same time, a gap state appeared below the Fermi level. No K-induced broadening in the UPS features was observed, indicating that the Pn SC thin films kept SC structure upon doping. The gap state was attributed to the occupied Mott-Hubbard band of the K_1Pn_1 Mott-Hubbard insulator. Such a band originated from the splitting of the half-filled LUMO band of K_1Pn_1 SC film, as induced by electron correlation effects. At 293 K, no impact of the K doping on the HOMO band dispersion was observed, and no dispersion for the gap state of the K_1Pn_1 SC multilayer was found. In contrast, at 50 K, a small but clear dispersion of the gap state (∼0.08 eV) of the K_1Pn_1 film was observed, which is in good agreement with the theoretical prediction for K_1Pn_1 Mott-Hubbard insulator crystal. Moreover, significant changes in the HOMO line shape in K-doped film were observed at 50 K, suggesting also the occurrence of a temperature-induced change in the intramolecular packing structure. The impact of K doping on the ELA was discussed in terms of coexistence of K_1Pn_1 Mott-Hubbard insulator and the Pn SC film. Independent of the doping level, no significant DOS was detected at the Fermi level, indicating stability of the Mott-Hubbard insulator ground state at least near the surface.

ACKNOWLEDGMENTS

This work was financially supported by the Global-COE Program of MEXT (G03: Advanced School for Organic Electronics, Chiba University) and Grant-in-Aid for Scientific Research (A; Grant No. 20245039).

*Corresponding author: fabio@restaff.chiba-u.jp
†uenon@faculty.chiba-u.jp

[1] C. W. Tang and S. A. VanSlyke, Appl. Phys. Lett. **51**, 913 (1987).
[2] J. H. Burroughes, D. D. C Bradley, A. R. Brown, R. N. Marks, K. Mackay, R. H. Friend, P. L. Burns, and A. B. Holmes, Nature (London) **347**, 539 (1990).
[3] C. D. Dimitrakopoulos and P. R. L. Malenfant, Adv. Mater. **14**, 99 (2002).
[4] T. Minakata, M. Ozaki, and H. Imai, J. Appl. Phys. **74**, 1079 (1993).
[5] A. B. Kaiser, Rep. Prog. Phys. **64**, 1 (2001).
[6] M. F. Craciun, S. Rogge, M. J. L. den Boer, S. Margadonna, K. Prassides, Y. Iwasa, and A. F. Morpurgo, Adv. Mater. **18**, 320 (2006).
[7] M. F. Craciun, G. Giovannetti, S. Rogge, G. Brocks, A. F. Morpurgo, and J. van den Brink, Phys. Rev. B **79**, 125116 (2009).
[8] P. J. Benning, J. L. Martins, J. H. Weaver, L. P. F. Chibante, and R. E. Smalley, Science **252**, 1417 (1991).
[9] M. Fahlman, D. Beljonne, M. Logdlund, R. H. Friend, A. B. Holmes, J. L. Brédas, and W. R. Salaneck, Chem. Phys. Lett. **214**, 327 (1993).
[10] H. Ding and Y. Gao, Appl. Phys. Lett. **92**, 053309 (2008).
[11] H. Ding and Y. Gao, Org. Electron. **11**, 1786 (2010).
[12] A. Hansson, J. Böhlin, and S. Stafström, Phys. Rev. B **73**, 184114 (2006).
[13] M. G. Betti, F. Crispoldi, A. Ruocco, and C. Mariani, Phys. Rev. B **76**, 125407 (2007).
[14] F. Evangelista, R. Gotter, N. Mahne, S. Nannarone, A. Ruocco, and P. Rudolf, J. Phys. Chem. C **112**, 6509 (2008).
[15] G. Iucci, K. Xing, M. Lögdlund, M. Fahlman, and W. R. Salaneck, Chem. Phys. Lett. **244**, 139 (1995).
[16] K. Z. Xing, M. Fahlman, M. Lögdlund, M. Berggren, O. Inganäs, M. R. Andersson, M. Boman, S. Stafström, G. Iucci, P. Broms *et al.*, Synth. Met. **80**, 59 (1996).
[17] G. Greczynski, M. Fahlman, W. R. Salaneck, N. Johansson, D. A. dos Santos, and J. L. Brédas, Thin Solid Films **363**, 322 (2000).
[18] P. J. Benning, D. M. Poirier, T. R. Ohno, Y. Chen, M. B. Jost, F. Stepniak, G. H. Kroll, J. H. Weaver, J. Fure, and R. E. Smalley, Phys. Rev. B **45**, 6899 (1992).
[19] F. Sunqi, Z. Xing, W. En, F. Jishi, M. Jinchang, G. Zhennan, Q. Jiuxin, Z. Xihuang, J. Zhaoxia, and Y. Bo, Solid State Commun. **80**, 639 (1991).
[20] Y. W. Park, Synth. Met. **56**, 3220 (1993).
[21] L. DeGiorgi, J. Low Temp. Phys. **105**, 1671 (1996).
[22] R. Mitsuhashi, Y. Suzuki, Y. Yamanari, H. Mitamura, T. Kambe, N. Ikeda, H. Okamoto, A. Fujiwara, M. Yamaji, N. Kawasaki *et al.*, Nature (London) **464**, 76 (2010).
[23] O. V. Molodtsova, V. M. Zhilin, D. V. Vyalikh, V. Yu. Aristov, and M. Knupfer, J. Appl. Phys. **98**, 093702 (2005).
[24] H. Yoshida and N. Sato, Phys. Rev. B **77**, 235205 (2008).
[25] S. D. Ha and A. Kahn, Phys. Rev. B **80**, 195410 (2009).
[26] H. Fukagawa, H. Yamane, T. Kataoka, S. Kera, M. Nakamura, K. Kudo, and N. Ueno, Phys. Rev. B **73**, 245310 (2006).
[27] S. Kera, H. Yamane, and N. Ueno, Prog. Surf. Sci. **84**, 135 (2009).
[28] D. V. Lang, X. Chi, T. Siegrist, A. M. Sergent, and A. P. Ramirez, Phys. Rev. Lett. **8**, 086802 (2004).
[29] J. Hwang, A. Wan, and A. Kahn, Mat. Sci. Eng., R **64**, 1 (2009).
[30] T. Sueyoshi, H. Fukagawa, M. Ono, S. Kera, and N. Ueno, Appl. Phys. Lett. **95**, 183303 (2009).
[31] E. Annese, J. Fujii, I. Vobornik, and G. Rossi, J. Phys. Chem. C **116**, 2382 (2012).
[32] S. Lukas, S. Söhnchen, G. Witte, and Ch. Wöll, ChemPhysChem **5**, 266 (2004).
[33] J. J. Yeh and L. Lindau, At. Data Nucl. Data Tables **32**, 1 (1985).
[34] N. Ueno, S. Kiyono, and T. Watanabe, Chem. Phys. Lett. **46**, 89 (1977).
[35] J. Cornil, D. Beljonne, J. P. Calbert, and J. L. Brédas, Adv. Mater. **13**, 1053 (2001).
[36] Y. C. Cheng, R. J. Silbey, D. A. da Silva Filho, J. P. Calbert, J. Cornil, and J. L. Brédas, J. Chem. Phys. **118**, 3764 (2003).

[37]C. C. Mattheus, G. A. de Wijs, R. A. de Groot, and T. T. M. Palstra, J. Am. Chem. Soc. **125**, 6323 (2003).
[38]H. Yamane, E. Kawabe, D. Yoshimura, R. Sumii, Y. Ouchi, N. Ueno, and K. Seki, Phys. Status Solidi **245**, 793 (2008).
[39]N. Ueno, S. Kera, K. Sakamoto, and K. Okudaira, Appl. Phys. A **92**, 495 (2008).
[40]N. Ueno and S. Kera, Prog. Surf. Sci. **83**, 490 (2008).
[41]N. Koch, A. Rajagopal, J. Ghijsen, R. L. Johnson, G. Leising, and J. J. Pireaux, J. Phys. Chem. B **104**, 1434 (2000).
[42]N. Koch, H. Oji, E. Ito, E. Zojer, H. Ishii, G. Leising, and K. Seki, Appl. Surf. Sci. **175**, 764 (2001).
[43]T. Schwieger, H. Peisert, M. Golden, M. Knupfer, and J. Fink, Phys. Rev. B **66**, 155207 (2002).
[44]M. Imada, A. Fujimori, and Y. Tokura, Rev. Mod. Phys. **70**, 1039 (1998).
[45]R. Eguchi, M. Taguchi, M. Matsunami, K. Horiba, K. Yamamoto, Y. Ishida, A. Chainani, Y. Takata, M. Yabashi, D. Miwa *et al*., Phys. Rev. B **78**, 075115 (2008).
[46]Y. Shichibu and K. Watanabe, Jpn. J. Appl. Phys. **42**, 5472 (2003).
[47]Y. Gao and L. Yan, Chem. Phys. Lett. **380**, 451 (2003).
[48]S. M. Sze, *Physics of Semiconductor Devices* (Wiley, New York, 1981), Sec. 1.4.2.